

# Numerical Study of Reduction of Ceiling Heat Load by Forced Convection

**Pattarawan Aimkamon<sup>a</sup>, Udomkiat Nontakaew<sup>b</sup> and Sudaporn Sudprasert<sup>c,\*</sup>**

<sup>a,c</sup> Faculty of Architecture and Planning, Thammasat University, Pathumthani 12121, Thailand

<sup>b</sup> Department of Mechanical Engineering, King Mongkut's Institute of Technology North Bangkok, Bangkok 10800, Thailand

## Abstract

The peak surface temperature of ceiling surface of a house in the hot and humid climate reaches 36-38 °C in the afternoon that causes uncomfortable condition and leads to high cooling energy consumption. Therefore, driving hot air off the attic by ventilation is a technique to reduce air and surface temperatures simultaneously. Using computational models in ANSYS Fluent and the average measured surface and air temperatures as the boundary conditions, this study investigated airflow and temperature reduction by forced convection produced by small exhaust fans and winglets. The three dimensional simulation model comprised of a vertical air gap connecting with a horizontal 10-cm air gap with dimensions of 3.0 m x 3.8 m x 0.13 m above the ceiling. Two fans of 680 m<sup>3</sup>/hour (100 Watts) placed at the two outlets at the soffit induced cool air of 25 °C from the ground floor flowing through the air channels and conveying heat out of the house. The validation of the simulation results was conducted by comparing with the previous experiments on horizontal air duct with hot surface facing down. The simulation results of exhaust fans turning on for 10 seconds showed the average air velocity in the horizontal channel increased to 1.0-1.5 m/s and air temperature reduced by 6.5-11.7 °C from 38.0 °C. The Installation of 2 rows of rectangular winglets with half air gap height, length of 30 cm and angle of attack of 45° increased the Nusselt number by 3 times of air gap without winglets. The vortices rotation enhanced convection heat transfer process near the winglets and decreased air temperature near surfaces by 2°C for 40 cm downstream from the rear tip of the winglets. Therefore, adopting of the system that consists of air gap formed by ceiling plates, the exhaust fans at the house soffits and two rows of winglets are preferable to reduce the effect of heat transfer in the attic.

\* Corresponding author.

E-mail: sudaporn@ap.tu.ac.th

**Keywords:** Forced convection, Attic, Winglets, Computational Fluid Dynamics, Hot and humid

## 1. Introduction

In the hot and humid climate, high ceiling surface temperature leads to higher cooling energy consumption and decrease thermal comfort. As an alternative ceiling insulation, removing hot air off the ceiling by natural and forced convection can be an effective technique to reduce room and surface temperatures (Petchdee & Chungloo, 2013, pp. 31-44). Attic ventilation was found to decrease cooling needs by 5% in the typical house with insulation (Parker, 2005). Insulation and radiant barrier in buildings in hot and humid climate bring about a problem of material deteriorate due to moisture. The proposed forced ventilation is an alternative controllable method to remove heat from the ceiling and the cost analysis is currently excluded in this study. The appropriate mechanism of extracting heat from the roof attic in the Malaysia weather was hybrid ventilation using ventilator driven by a solar panel (Al-Obaidi, Mazra & Rahman, 2014). In Thailand, general houses utilize the soffit vents but the soffits could not remove heat from the attic effectively and the ceiling surface temperature increased up to 36-38°C in the afternoon.

Free convection study showed that the cool air entered a room through openings and left through the hot horizontal attic was ineffective (Ziskind, Dubovsky & Letan, 2002). The inclined air gap incorporated with the inclined roof showed low airflow rate under the free convection process (Hirunlabh, Wachirapuwadon, Pratithong & Khedari, 2001; Bunnag, Khedari, Hirunlabh & Zeghami, 2004). The roof with air gap showed results in the coolest attic comparing to conventional tile roof, but the air temperature in the attic of 35-40°C was high during the peak hours (Ong, 2011). Therefore, the low air temperature flowing in the air gap to extract heat from roof and ceiling surfaces was required. In the free convection, the Nusselt number in the range of 2-40 and air velocity of 0.0-0.5 m/s found in the experiment of open-ended inclined channels (Azevedo & Sparrow, 1985) was not enough to remove heat from the channel. Comparing to the forced convection applied with winglets, the Nusselt number were 155-245 for Reynolds number of  $2 \times 10^4$  (Moon & Lau, 2003).

In addition to the forced convection by fans, installed winglets obstruct the flow and enhance convection heat transfer in the solar air heaters by creating swirling air (vortex) to capture heat from the absorber plate and remove heat through warm air from the heater. Winglets were found in various shapes, i.e., rectangular, trapezoid, delta and curved trapezoid (Zhou & Ye, 2012), twisted

rings (Thianpong, Yongsiri, Nanan & Eiamsa-ard, 2012), arranged in parallel configuration or 15-60° (Han & Zhang, 1991) with the direction of the main flow. The results of computed surface Nusselt number with the winglets ( $Nu$ ) in air heaters were found higher than the Nusselt's number in the smooth air heaters by 0.8-3.6 times for the Reynold's number ( $Re$ ) of  $4,400-5 \times 10^4$  (Hwang & Liou, 1995; Sara, Pekdemir, Yapici & Yilmaz, 2001; Bekele, Mishra & Dutta, 2011). In this study the Reynold's number was in the range of 9,600-28,000 similar to the previous studies. The purpose of this paper are: (1) to investigate the number of exhaust fans and installation positions to induce cool air from the first floor of the house into the air gap above the ceiling; and (2) to study the influence of width, height, location and angle of attack of the rectangular winglets in the air gap aiming to design the air gap with high Nusselt number and reduction of air temperature adjacent to the surfaces in air gap.

## 2. The Simulation Models

### 2.1 The Geometrical Model

The 3D simulation models were constructed in the Rhinoceros 4.0 and exported to the CFD program ANSYS Fluent 14.0. The room wall and the added outer skin formed a vertical air gap of height 3.22 m. and width 3.0 m. The room ceiling and the added horizontal panel formed a horizontal air gap of length 3.9 m. and width of 3.0 m. above the room ceiling as shown in Figure 1a. The vertical and horizontal air gaps were connected as an airflow channel with height ( $H$ ) of 0.10 m. The inlet located at the stair hall and the outlets located externally at the exterior soffit. The dimensions of air gap were derived from a room in a generic two-floor house in Thailand shown in Figure 1b. The installation of exhaust fans at the outlet of the horizontal air gap as shown in Figure 2 was expected to draw sufficient cool air. However, the number of fans and positions influencing the airflow rates and air temperature need proper specification.

### 2.2 The numerical solution

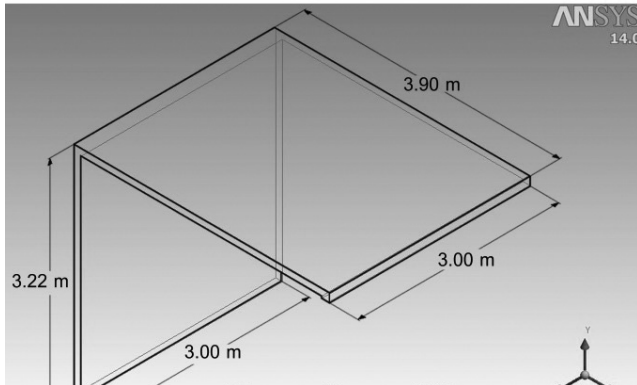
The numerical calculations were performed to solve the following steady state equations:

- continuity

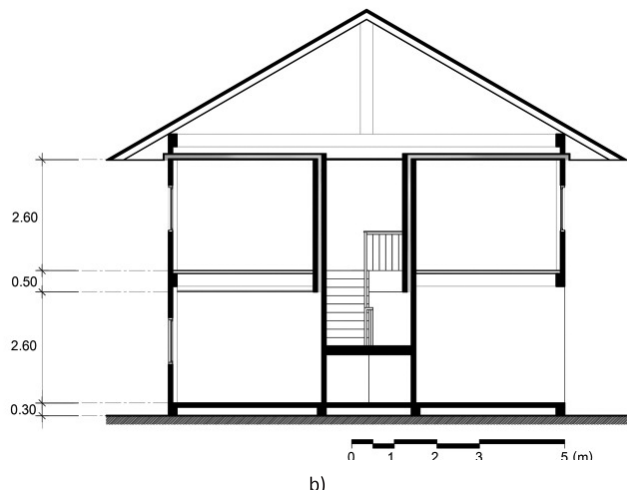
$$\frac{\partial}{\partial x_i} (\rho u_i) = 0 \quad (1)$$

- momentum

$$\frac{\partial}{\partial x_i} (\rho u_i u_j) = \frac{\partial p}{\partial x_i} + \frac{\partial \tau_j}{\partial x_i} + \rho g_i \quad (2)$$



a)



b)

**Figure 1.** The geometrical model of (a) the air channel connecting first floor and the ceiling and (b) the two-floor house.

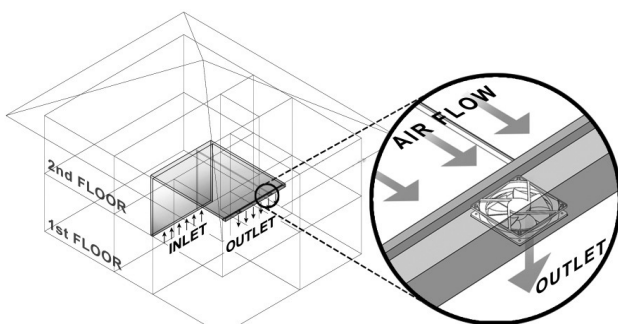


**Figure 2.** Position of ventilation fan in the studied model.

- energy

$$\frac{\partial}{\partial x_i} (\rho u_i h) = \frac{\partial}{\partial x_i} \left( k \frac{\partial T}{\partial x_i} \right) + u_i \frac{\partial p}{\partial x_i} + \tau_i \frac{\partial u_i}{\partial x_j} \quad (3)$$

where  $\rho$  is the density,  $u_i$  the velocity component in the  $i$ -direction,  $p$  the static pressure,  $x_i$  a Catesian coordinate,  $\tau_{ij}$  the stress tensor,  $g_i$  the gravitational acceleration in the  $i$ -direction,  $h$  the static enthalpy,  $k$  the thermal conductivity and  $T$  is the temperature. Since the flow was buoyancy driven under small temperature difference, the Boussinesq approximation was used with a constant air density. [Table 1](#) shows detail input to the computational model. The boundary conditions for the momentum equation were no-penetration, no-slip at all boundaries. When the exhaust fan was turned on, the gauge pressure at the inlet boundary was 0.0 Pascal and the pressure at the outlet was -87.87 Pascal. The outlet pressure was determined from pressure different of an exhaust fan of 340 m<sup>3</sup>/hour.

The boundary conditions for the energy equations were constant temperature on the hot plate such as roof, ceiling and added plates on the wall and above the ceiling. The ambient temperature of 28.5°C, inlet and outlet air temperatures of 25°C were adopted from field measurement of a two-floor house with enclosed attic space shown in [Figure 1b](#). The measured wall, ceiling exterior surface, and ceiling interior surface temperatures of 30.5°C, 38°C and 36°C were assumed for vertical surfaces (W1 and W2), and exterior and interior horizontal (H1 and H2) surfaces of the air gap in the simulation model, respectively. The SIMPLE algorithm were used for pressure-velocity coupling. In all study cases, the converged solutions were obtained from 3,000 iterations.

### 2.3 Mesh independency analysis

The mesh size and the number of mesh could influence the simulation results. In this study, the mesh cells in the problem domain were varied from 566,107 to 1,584,010. [Figure 3](#) shows that the model with mesh number of 1,019,334 gave results of temperature and velocity fields similar to the results from model with mesh number of 1,584,010. Therefore, the mesh number around 1,100,000 was used in the simulation models.

## 3. Simulation Results

### 3.1 Natural ventilation in the air channel

The proposed design air gap with fan turned off was

| Procedure  | Input  |
|--|--|
| <b>Geometry</b>                                  |  |
| Import model                                     | Import file .stp from Rhinoceros                         |
| <b>Mesh</b>                                      |  |
| Number of mesh                                   | 1,100,000  |
| <b>Setup</b>                                     |  |
| Gravity (x,y,z)                                  | 0, - 9.81, 0 m/s <sup>2</sup>                            |
| Time   | Steady   |
| Viscous Model                                    | RNG k-e, Enhance wall Treatment<br>Full Buoyancy Effects |
| <b>Materials Properties</b>                      |  |
| Density (kg/m <sup>3</sup> )                     | 1.17 (Boussinesq model)                                  |
| Thermal Expansion Coefficient (K <sup>-1</sup> ) | 0.003315   |
| Specific Heat (J/kgK <sup>-1</sup> )             | 1007   |
| Thermal Conductivity (W/mK)                      | 0.025769   |
| Viscosity (m <sup>2</sup> /s)                    | 1.8651 x 10e-5   |
| <b>Boundary Conditions</b>                       |  |
| Inlet (Type: Pressure Inlet)                     | guage pressure = 0 Pascal                                |
| Outlet (Type: Pressure Outlet)                   | guage pressure = -87.8675 Pascal                         |
| Temperature of wall, Roof, ceiling               | 30.5 °C, 38 °C, 36 °C                                    |
| <b>Solutions Method</b>                          |  |
| Pressure-Velocity Coupling                       | SIMPLE   |
| Spatial Discretization                           |  |
| Gradient   | Least Square Cell Based                                  |
| Pressure   | PRESTO!  |
| Momentum   | Second Oder Upwind                                       |
| Turbulent Kinetic Energy                         | Second Oder Upwind                                       |
| Turbulent Dissipation Rate                       | Second Oder Upwind                                       |

Table 1. The input of ANSYS Fluent program.

| Number of fans | Average air velocity (m/s) | Average temperature (°C) |
|----------------|----------------------------|--------------------------|
| 0              | 0.05                       | 34.21                    |
| 1              | 1.01                       | 29.17                    |
| 2              | 1.50                       | 28.57                    |
| 3              | 2.06                       | 28.24                    |

Table 2. Number of fans installed opposite to the inlet and the results of average air velocity and temperature in the air gap.

expected to generate natural ventilation due to the buoyancy effect. The results of simulated model in this study under natural ventilation are shown in Figure 4. The average air velocity in the vertical air gap is 0.03 m/s and in the horizontal air gap is 0.05 m/s. The higher velocity in the horizontal air gap due to higher temperature. The temperature of surfaces W1 and W2 is only 5°C higher than the inlet air temperature, which brings about slight buoyancy effect and air velocity. In addition, the facing down warm surface H2 of the horizontal air gap keeps warm air trapped under the surface H2 and decelerates the outflow. In detail, high air velocity of 0.5-0.7 m/s were found in the vicinity of surface H1 near the downward outlet.

Figure 5 shows that the temperature stratification of warm air in the air gap, characterized the natural ventilation from buoyancy effect. The air temperature of 32-36°C are found in the horizontal air gap beside the surface H1. Comparing to the warm surface H2 with temperature of 38°C, the air in the horizontal air gap of 32-36°C translating to lower heat gain. However, the air temperature is too high to provide comfortable condition in the room below the ceiling. The exhaust fans investigated in the next section would draw more air of 25-30°C from the vertical air gap to the horizontal air gap.

### 3.2 The effect of number and positions of fans on airflow and temperature distribution

Figures 6a-6c showed the simulation results of 1, 2 and 3 exhaust fans installation at the outlet of horizontal air gap opposite to the inlet. Assuming exhaust fans are identical, increase of number of fans enhances the volume flow rate. The increase of number of fans from 1 fan to 2 and 3 fans raises the average velocity from 0.5 m/s to 1.3 and 2.0 m/s, however, the temperature patterns and ranges are unchanged. The average air temperature and velocity of 1, 2, 3 fans opposite to the inlet are shown in Table 2.

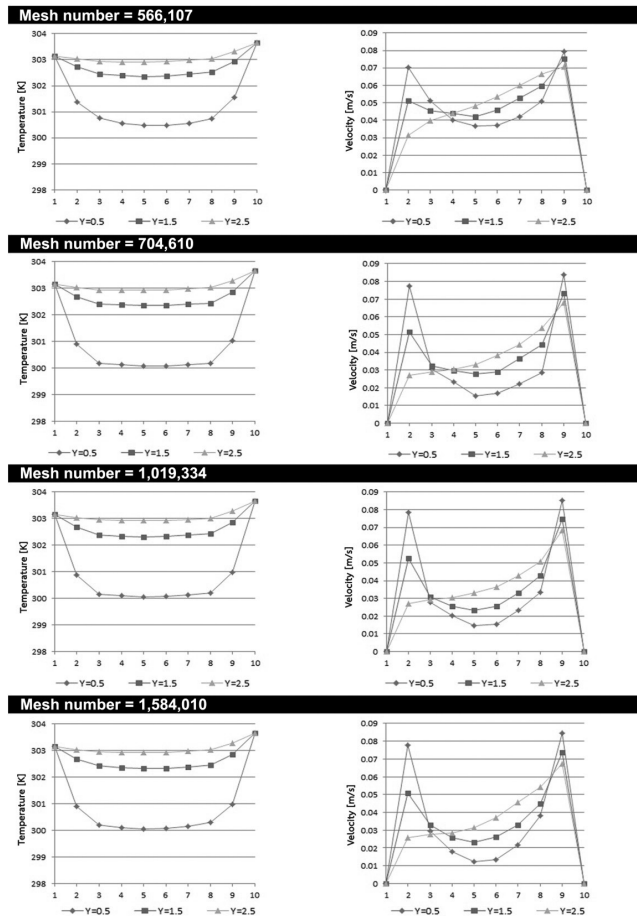


**Figure 3.** Mesh independence analysis shows temperature and velocity distribution across the vertical channel at coordinate  $y= 0.5, 1.5$  and  $2.5$  m.

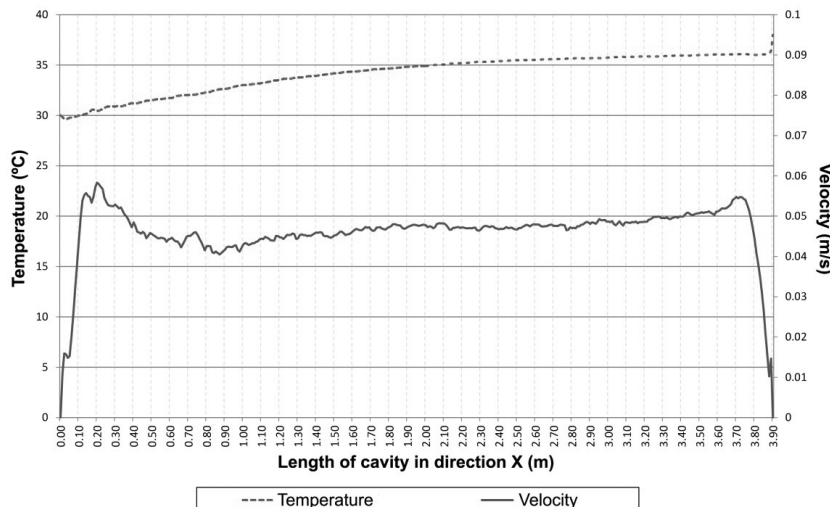


**Figure 4.** Temperature and velocity distribution in the air gap.

The installation of fans at the positions perpendicular to the inlet creates transverse vortex whose rotation axis normal to the main flow as shown in [Figure 7a](#). The transverse vortex obstructs air to flow and causes increase in air temperature. The increase of number of fans can overcome the transverse vortex but the penalty of air velocity reduction in the remote regions occurs as shown in [Figure 7b](#) and [7c](#).

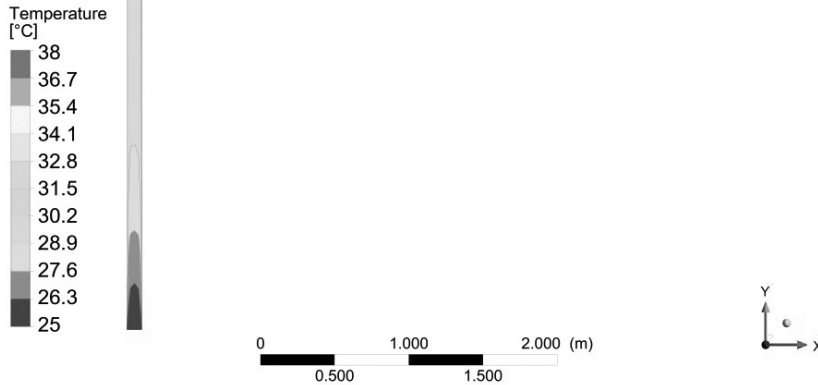
[Figure 8](#) shows graphs of air velocity and air temperature in the horizontal air gap at  $y=3.17$  m. One exhaust fan pull cool air along the horizontal air gap to the length of 2.4 m. with velocity of 0.7 m/s. The air velocity increases to 4.0 m/s near the fan located opposite to the inlet, in contrast to the fan located perpendicular to the inlet, the air velocity drops to 0.05 m/s. The generating of large transverse vortex results into the increase of air temperature from 26.0°C to 36.5°C or 10°C. Comparing to the fan opposite to inlet, temperature linearly increases gradually from 26.5°C to 30°C. Therefore, the installation of fans opposite to the inlet is preferable in both air velocity and air temperature in the gap.

### 3.3 Design of winglets to enhance convection heat transfer

#### 3.3.1 The effect of winglet aspect ratio

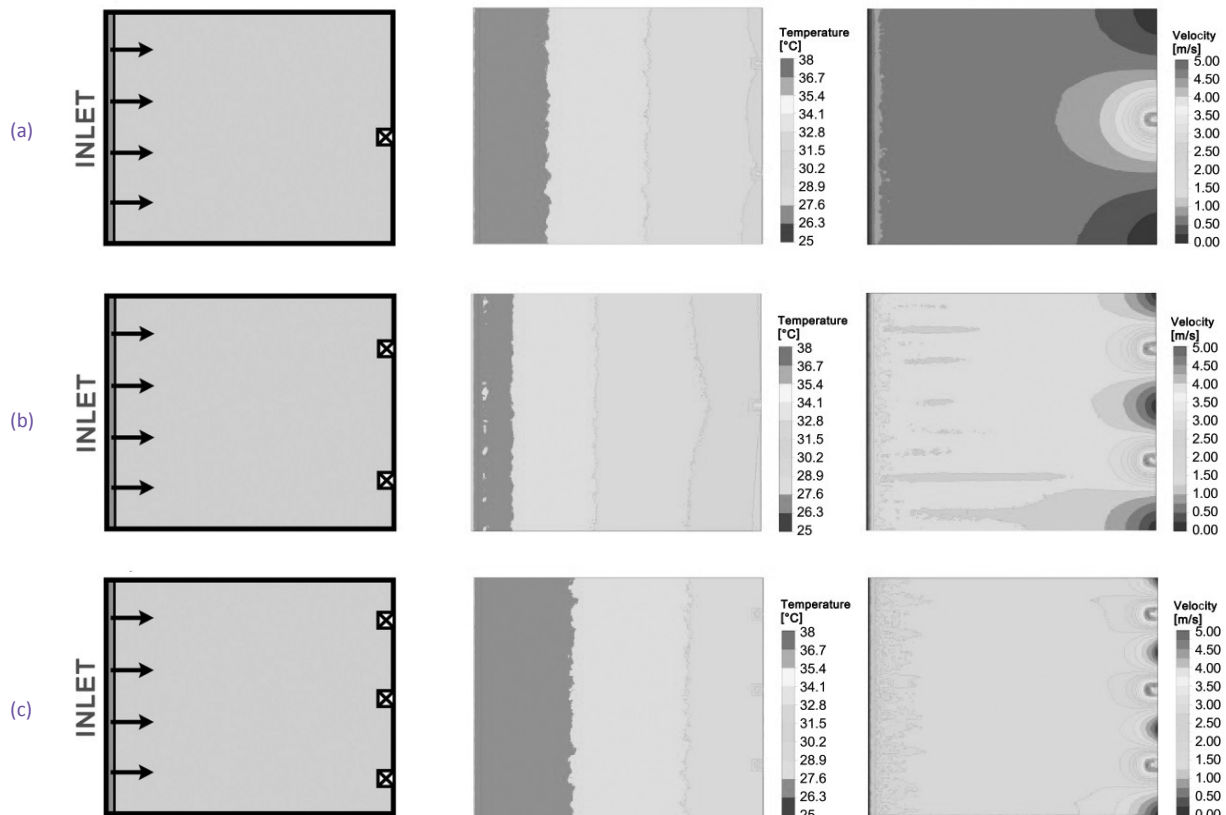
The winglet aspect ratio is the ratio of  $b^2/S$  where  $b$  is the winglet span and  $S$  is the winglet height. The winglet with appropriate aspect ratios generate longitudinal vortices behind its trailing edge and strong vortices for far distance from the winglet. To study the effect of winglet height, three primary simulation models include rectangular winglet

attached to the horizontal surface H2 at distance  $x=2.5$  m. from the entrance with angle of attack of  $15^\circ$  as shown in [Figure 9](#). The height of studied winglets were 0.025 m., 0.050 m. and 0.075 m., i.e.,  $0.25H$ ,  $0.5H$  and  $0.75H$ , respectively. [Figure 10](#) shows the simulation results of temperature and Nusselt number distribution oversurface H2. Qualitatively, the temperature distribution on surface H2 with and without winglet are similar, except in the vicinity of the winglet. Without winglet, the minimum surface temperature of  $25^\circ\text{C}$  is located near the entrance at the coordinate  $(0, 3.2, 1.5$  m.) and air temperature increases to  $30.5^\circ\text{C}$  for  $2.70 \text{ m.} < x < 3.70 \text{ m.}$  With the winglet, the swirling flow behind the winglet ( $x > 2.60 \text{ m.}$ ) decreases air temperature in region of winglet downstream to  $29.6^\circ\text{C}$ . The results of Nusselt number corresponds with



[Figure 5](#). The stratification of warm air in the vertical and horizontal air gap.

[Figure 6](#). Sections of horizontal air gap show results of temperature and velocity distribution in the model with (a) 1 fan, (b) 2 fans and (c) 3 fans installation opposite to inlet.



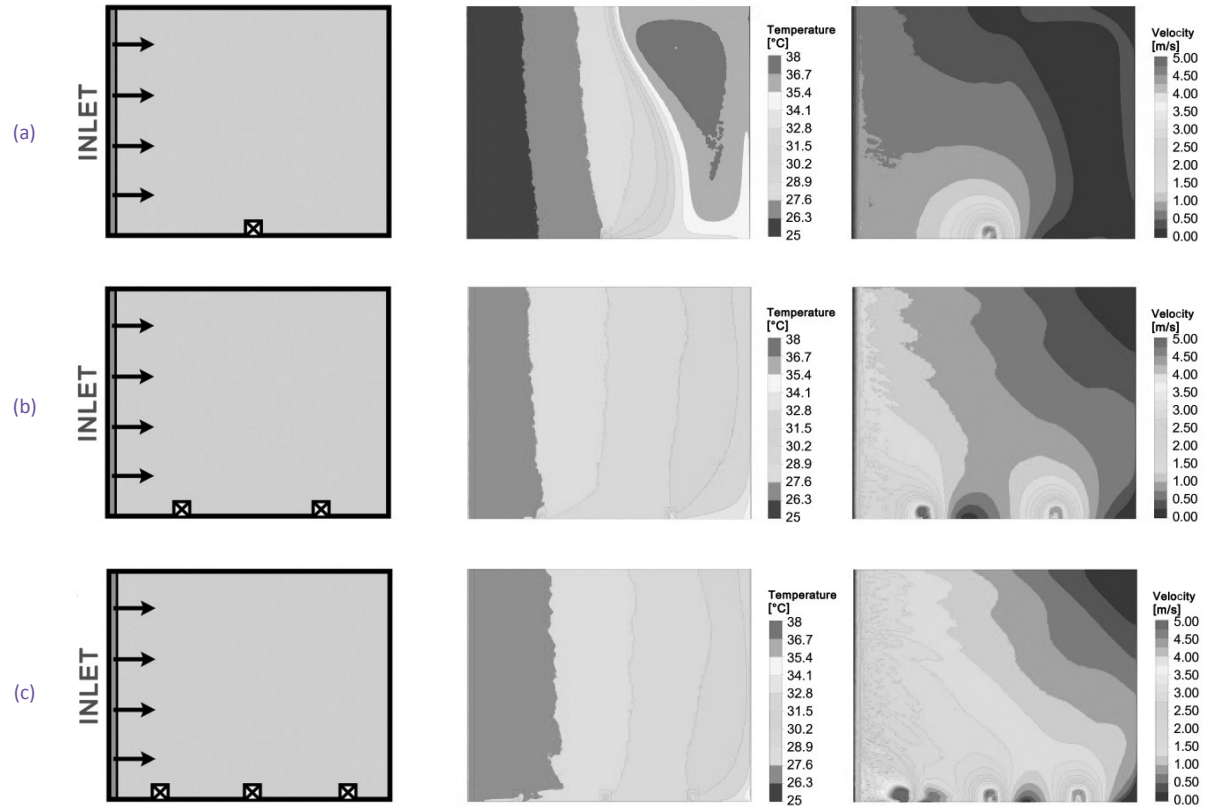


**Figure 7.** Sections of horizontal air gap show results of temperature and velocity distribution in the model with (a) 1 fan, (b) 2 fans and (3) 3 fans installation perpendicular to inlet.

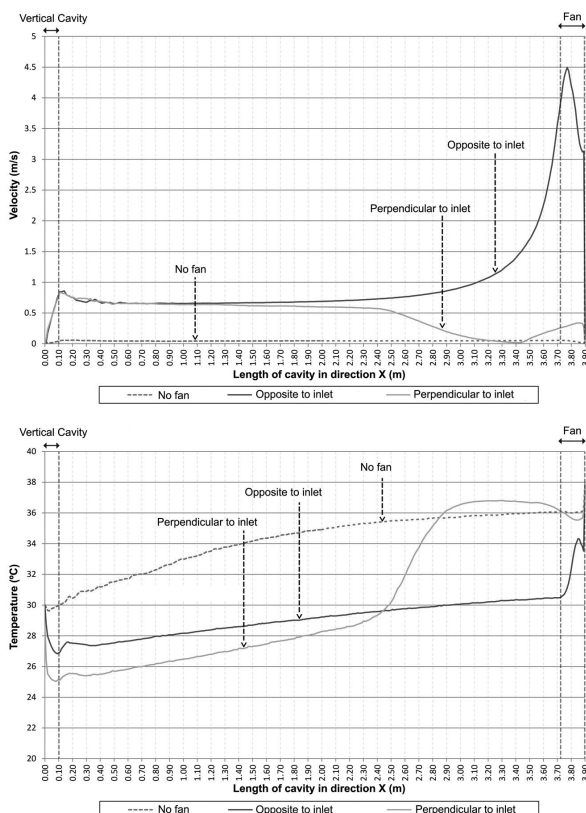


**Figure 8.** Comparison of a) velocity and b) air temperature along the horizontal air gap without fan, with 1 fan opposite to inlet and with one fan perpendicular to inlet.

results of air temperature. Comparing to surface H2 without winglets with Nusselt number of 240, the surface H2 with winglet enhances the heat transfer from surface to air and increases the Nusselt number to 300-310.

To choose proper winglet height, analysis of vortex form and vortex strength are also needed. Shown in **Figure 11a**, the result of velocity vector and air temperature contour in the air gap at  $x = 2.55$  m. The winglet with height of  $0.5H$  develops circular vortex close to surface H2 where the vortex collect heat and carry away to the outlet. The winglet with height of  $0.25H$  creates incomplete circular vortex and the vortex created by the winglet with  $0.75H$  locates far from the surface H2. The mixing of warm

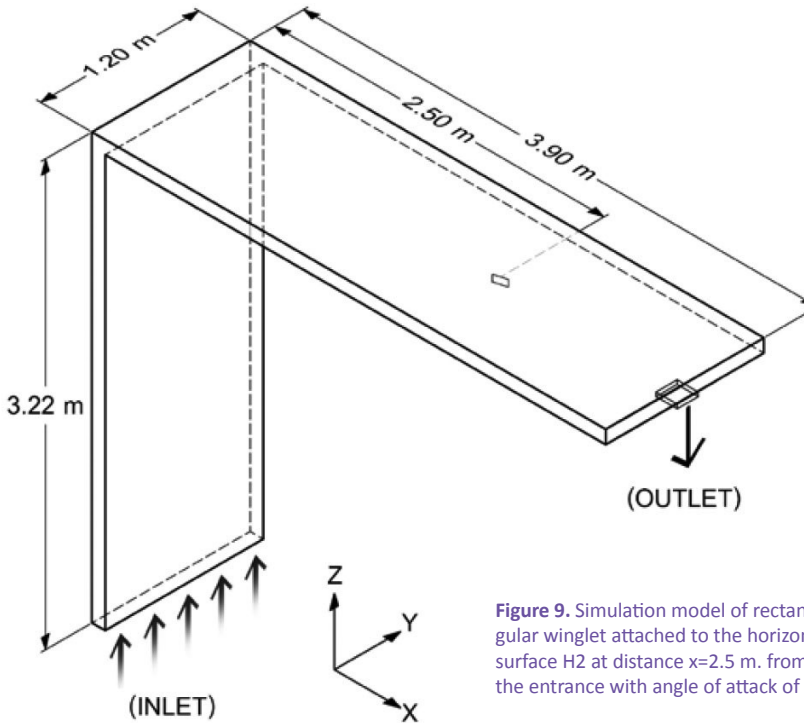


Figure 9. Simulation model of rectangular winglet attached to the horizontal surface  $H_2$  at distance  $x=2.5$  m. from the entrance with angle of attack of  $15^\circ$ .

Figure 10. Temperature and Nusselt number distribution along the horizontal air gap at  $z=0.6$  m.

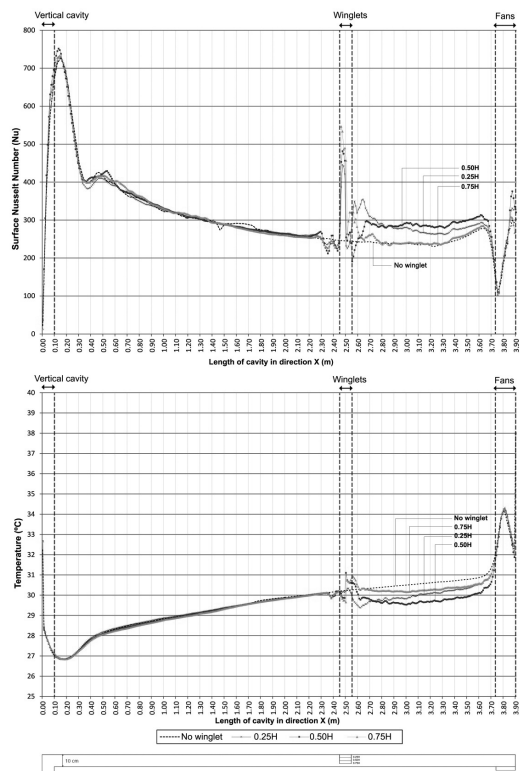
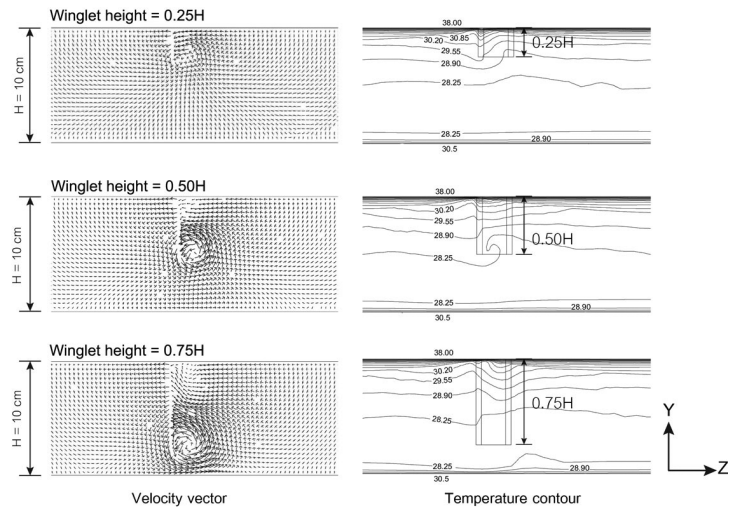


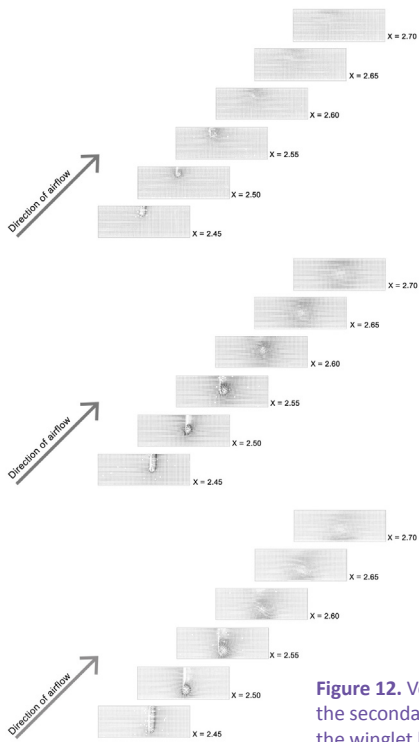
Figure 11. Development of (a) velocity vector (b) temperature contour behind the winglet with  $0.25H$ ,  $0.5H$  and  $0.75H$  at  $x=2.55$  m.



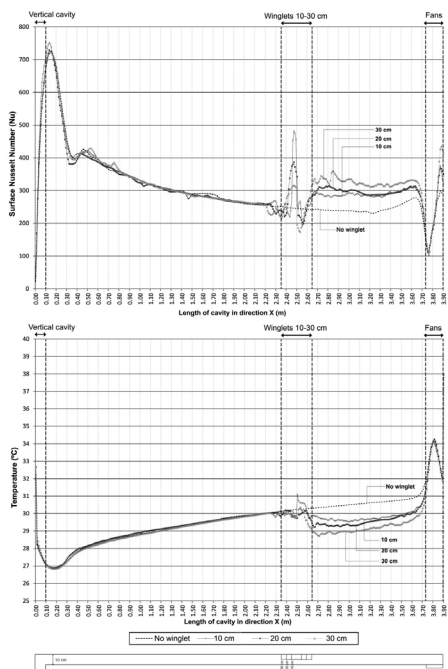
air and the cool inflow air occurs at upper part of the air gap help separate the too warm air from the surface  $H_1$ , as shown in Figure 11b. Therefore, the winglet with  $0.5H$  provides effective heat transfer enhancement.

Figure 12 compares strength and form of vortices generated by winglet with height of  $0.25H$ ,  $0.5H$  and  $0.75H$ . In Figure 12, the form of longitudinal vortices changes from section to section and depends on winglet height. From near the winglet to far downstream, the shape of vortices generated by the winglet with height of  $0.25H$  changes from circular to flat and appears at section  $x=2.70$  m. The shapes of vortices generated by the winglets with height of  $0.5H$  and  $0.75H$  show less change in their shapes and keep nearly in circular form for  $2.45$  m.  $< x < 2.75$  m. Hence, the winglet with height of  $0.5H$  is selected for the next study of winglet span.

To study the effect of winglet span, the winglet models with height  $0.5H$  and span of  $0.1$  m.,  $0.2$  m. and  $0.3$  m. were simulated for angle of attack of  $15^\circ$ . Figure 13 compares the results of spanwise Nusselt number distribution and air temperature near surface  $H_2$ .



**Figure 12.** Velocity vectors of the secondary flow generated by the winglet height of (a) 0.25H (b) 0.5H and (c) 0.75H in seven y-z planes of  $x= 2.45, 2.50, 2.55, 2.60, 2.65, 2.70, 2.75$ , respectively.



**Figure 13.** Distribution of Nusselt number and air temperature for air gap without winglet and with winglet with spans of 0.1 m., 0.2 m. and 0.3 m.

It shows that the increase of winglet span improves the Nusselt number to 290-300. The air temperature near surface H2 reduces to 29-30°C by applying the winglet span of 0.3 m. From the simulation results in this study, the winglet with aspect ratio of  $0.30^2/0.05 = 1.8$  provides the best heat transfer enhancement.

### 3.3.2 Influences of angle of attack

The aspect ratio of the winglet is 1.80 taken from the previous results to study the angle of attack in this section. **Figure 14** shows the results of spanwise average Nusselt number and air temperature of the investigated angles of attack ( $\beta$ ) of 15°, 30°, 45° and 60°. The peak value of Nusselt number for the winglet with  $\beta=45^\circ$  is highest, followed by that of  $\beta=30^\circ$ ,  $\beta=60^\circ$  and  $\beta=15^\circ$ , respectively. For all  $\beta$ , the Nusselt number drops to 310 at  $x=3.60$  m.

The simulation results along the air gap at  $x=2.7$  m. show the appropriate attack angle are 30° and 45°. However, less number of winglets are required in the installation of 45° winglets compared to those of 30° winglets. Therefore, the winglet with angle of attack=45° is a selected for arrangement in rows in the next section.

### 3.3.3 Influences of winglet arrangements

For the winglet with aspect ratio of 1.8 and attack angle of 45°, two patterns of winglet rows: the V-pattern and the parallel pattern, were attached on the warm surface facing down (H2 plate) at  $x=2.5$  m. as shown in **Figure 15**. The surface temperature of H2 and H1 were 38°C and 30.5°C, respectively. The result of Nusselt number distribution are shown in **Figure 16**. The V-pattern gives higher Nusselt number of 300-650 in the area behind the winglets than those of 250-500 in the parallel pattern. Therefore, the V-shape pattern is recommended in practice.

## 4. Conclusions

This work presents a numerical study of forced convection enhancement to reduce heat load in the attic of a generic two-floor house. The horizontal air gap of 10 cm height constructed above the ceiling was connected with the vertical air gap to pull cool air of 25°C from the first floor. The simulation results showed that free convection along the air gap, developed by temperature difference, removed warm air of 36-38°C out of the ceiling inefficiently. To increase the cool air flow, small fans are installed at the outlet of the air gap. For the ceiling area of  $3.0 \times 3.9 \text{ m}^2$ , two fans of  $680 \text{ m}^3/\text{hour}$  located opposite to

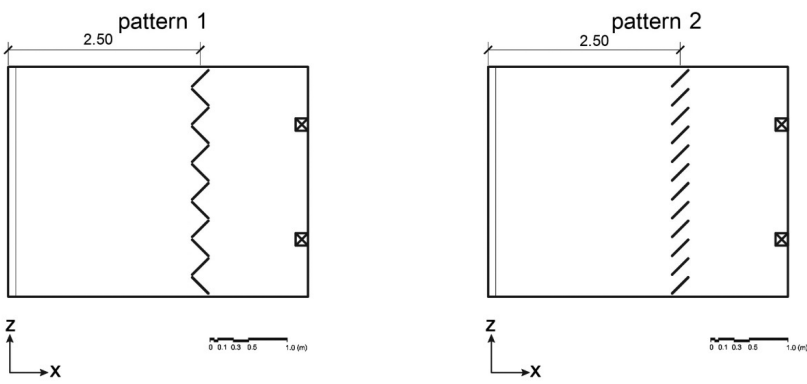


Figure 15. The winglet arrangements.

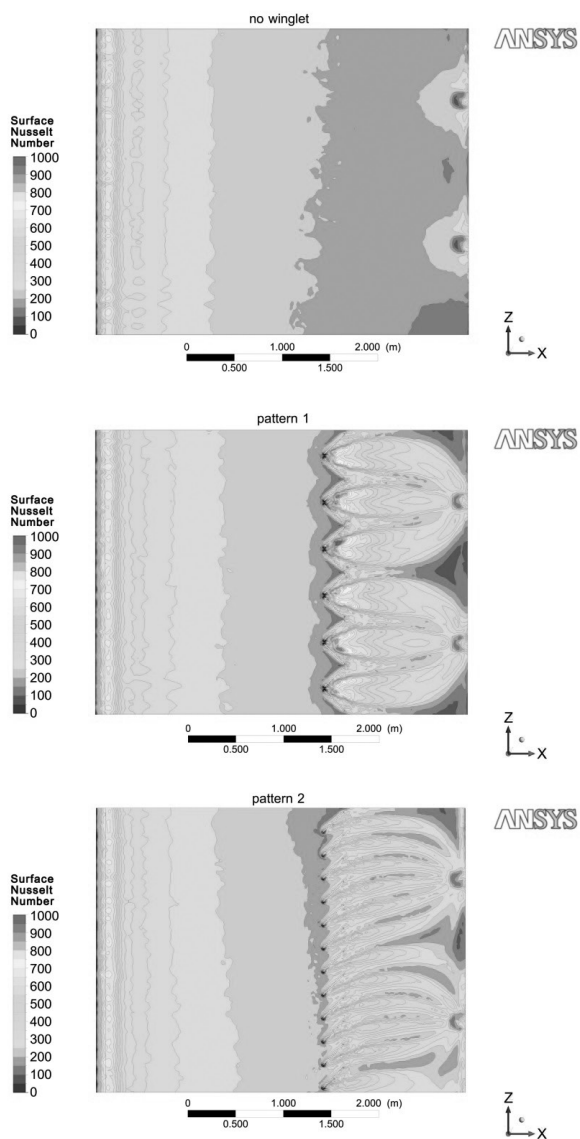


Figure 16. The simulation results of Nusselt number distribution without winglet, with winglet of V-shape arrangement and parallel arrangement.

the inlet of the horizontal air gap are recommended. These fans provided average air velocity of 1.5 m/s and air adjacent to ceiling surface was around 31.0°C. The designed air gap with fans perform an active insulator that could be an alternative to the conventional insulation materials. To increase the heat transfer from the air gap, two rows of rectangular winglets were suggested to carefully attach on the warm surface of the air gap. The rectangular winglet of 0.5H, aspect ratio of 1.8, attack angle of 45° arranged in the v-pattern is recommended here. The simulation results show that Nusselt number in the air gap with winglets increase by 3.45 times compared to those without the winglets. As the Nusselt number represents convective heat transfer to the conductive heat transfer across the boundary layer, the increase of Nusselt number bring positive effect on the ceiling temperature. It was found that, with the winglet installation, the average temperature of air adjacent to the surface further reduces to 28.5°C.

## 5. Acknowledgement

This research was partially supported by the research fund from Faculty of Architecture and Planning, Thammasat University. The author also would like to thank the Research Centre for Advanced Computational and Experimental Mechanics (RACE), KMUTNB for provision of ANSYS Fluent computational program and technical support throughout the research.

## References

Al-Obaidi, K. M., Mazra, I. & Rahman, A. M. A. (2014). A review of the potential of attic ventilation and active turbine ventilators in tropical Malaysia. *Sustainable Cities and Society*, 52, 232-240.

Azevedo, L. F. A. & Sparrow, E. M. (1985). Natural convection in opened-ended inclined channels. *Journal of Heat Transfer*, 107, 893-901.

Bekele, A., Mishra, M. & Dutta, S. (2011). Effects of delta-shaped obstacles on the thermal performance of solar air heater. *Advanced Mechanical Engineering*, 1-10.

Bunnag, T., Khedari, J., Hirunlabh, J. & Zeghami, B. (2004). Experimental investigation of free convection in an open-ended inclined rectangular channel heated from the top. *Ambient Energy*, 25, 151-162.

Han, J. C. & Zhang, Y. M. (1991). High performance heat transfer ducts with parallel broken and V-shape broken ribs. *International Journal of Heat and Mass Transfer*, 35, 513-29.

Hirunlabh, J., Wachirapuwadon, S., Pratinthong, N. & Khedari, J. (2001). New configuration of a solar collector maximizing natural ventilation. *Building and Environment*, 36, 383-391.

Hwang J. J. & Liou, T. M. (1995). Heat transfer in a rectangular channel with perforated turbulence promoters using holographic interferometry measurement. *International Journal of Heat and Mass Transfer*, 38, 3197-207.

Moon, S. W. & Lau, S. C. (2003). Heat transfer between blockages with holes in a rectangular channel. *J. Heat Transfer*, 125(4) 587-593.

Ong, K. S. (2011). Temperature reduction in attic and ceiling via insulation of several passive roof design. *Energy conversion and Management*, 52, 2405-2411.

Parker, D. S. (2005). *Literature review of the impact and need for attic ventilation in Florida homes*. Florida, USA: Florida Solar Energy Center.

Petchdee, P. & Chungloo, S. (2013). Improvement of louvers and openings of factory building to remove heat through natural wind. *Journal of Architectural/Planning Research and Studies*, 10(2), 31-44.

Sara, O. N., Pekdemir, T., Yapici, S. & Yilmaz, M. (2001). Heat transfer enhancement in a channel flow with perforated rectangular blocks. *Heat and Fluid Flow*, 22, 509-18.

Thianpong, C., Yongsiri, K., Nanan, K. & Eiamsa-ard, S. (2012). Thermal performance evaluation of heat exchangers fitted with twisted-ring turbulators. *International Communications in Heat and Mass Transfer*, 39, 861-68.

Zhou, G. & Ye, Q. (2012). Experimental investigations of thermal and flow characteristics of curved trapezoidal winglet type vortex generators. *Applied Thermal Engineering*, 37, 241-48.

Ziskind, G., Dubovsky, V. & Letan, R. (2002). Ventilation by natural convection of a one-story building. *Energy and Buildings*, 34, 91-102.

